Calcium Pump Kinetics Determined in Single Erythrocyte Ghosts by Microphotolysis and Confocal Imaging

Ulrich Kubitscheck,* Lothar Pratsch,* Hermann Passow,‡ and Reiner Peters*

*Institute of Medical Physics and Biophysics, Westfälische Wilhelms University, 48149 Münster, and ‡Max Planck Institute of Biophysics, 60528 Frankfurt, Germany

ABSTRACT The activity of the plasma membrane calcium pump was measured in single cells. Human red blood cell ghosts were loaded with a fluorescent calcium indicator and either caged calcium and ATP (protocol A) or caged ATP and calcium (protocol B). In a suitably modified laser scanning microscope either calcium or ATP were released by a short UV light pulse. The time-dependent fluorescence intensity of the calcium indicator was then followed in single ghosts by repetitive confocal imaging. The fluorescence intensity was converted into calcium concentration, which in turn was used to derive the kinetic parameters of the calcium pump, the Michaelis-Menten constant K_m, and the maximal transport rate v_{max}. K_m and v_{max} values derived in this manner were 24 ± 14 μM and 1.0 ± 0.6 μM/(ghost s) for protocol A, and 4 ± 3 μM and 1.0 ± 0.6 μM/(ghost s) for protocol B, respectively. The difference between A and B is presumably caused by calmodulin, which is inactive in the experiments with protocol A. The possibilities to extend the new method to living nucleus-containing cells transiently transfected with mutants of the plasma membrane calcium pump are discussed.

INTRODUCTION

The plasma membrane calcium pump (PMCA, reviewed by Garrahan and Rega, 1990; Strehler, 1991; Carafoli, 1992) plays an important role in cellular calcium homeostasis and signaling (reviewed by Bonventre, 1992; Petersen et al., 1994). Although discovered and initially characterized in the erythrocyte membrane (Schatzmann, 1966), the PMCA was found to be ubiquitous among eukaryotic cells, and several isoforms have been cloned and sequenced from both humans and mice (Shull and Greeb, 1988; Verma et al., 1988). All of these isoforms are large proteins containing approximately 1200 amino acid residues with a total mass of 130 kDa. Secondary structure predictions (reviewed by Carafoli, 1991) suggest that the PMCA, similar to the calcium pump of the sarcoplasmic reticulum (SERCA, MacLennan et al., 1985), harbors 10 transmembrane domains. The vast majority of the molecular structure (~80%), however, is exposed on the cytoplasmic membrane face forming three functional units for ATP binding, energy transduction, and a calmodulin interaction, respectively.

Functional parameters of the PMCA such as transport kinetics, energy dependence, and regulation by magnesium ions, lipids, and calmodulin have been studied most commonly in erythrocyte ghosts (e.g., Kratje et al., 1985). When erythrocytes are lysed at 0°C in a medium of tightly controlled ion composition and pH (Schwoch and Passow, 1973) they become freely permeable for small and large molecules. Thus, the natural intracellular constituents, in particular hemoglobin, are released and the extracellular medium is taken up. Subsequently the erythrocyte membranes can be resealed by warming them in an isotonic medium. Calcium ion transport can be sensitively measured by using ^{45}Ca as a tracer. By these and other means it has been established that the PMCA belongs to the P-type ion pumps (Pedersen and Carafoli, 1987a,b) for which the formation of a phosphorylated intermediate and the inhibition by orthovanadate is characteristic. It is generally assumed that the detailed kinetic schemes that have been proposed for the mechanism of the SERCA (Jencks, 1989, 1992) and other P-type pumps (Becker, 1994) are also essentially valid for the PMCA. A distinct difference, however, seems to exist in the stoichiometry between transported calcium ions and hydrolyzed ATP, which is two in the SERCA but apparently one in the PMCA.

The method described in this paper is based on the combination of fluorescence microphotolysis (Peters et al., 1974; reviewed in Peters and Scholz, 1991) with confocal laser scanning microscopy. As shown schematically in Fig. 1, human erythrocyte ghosts were loaded with a fluorescent calcium ion indicator and either ATP and caged calcium or calcium and caged ATP. Confocal laser scanning microscopy was employed to image and quantify the fluorescence inside single ghosts. The PMCA was activated by microphotolysis of the caged compounds with the high pressure mercury lamp of the microscope. The time-dependent intracellular fluorescence was converted into calcium ion concentration, and this was fitted by the numerically integrated Michaelis-Menten equation to derive values for the Michaelis-Menten constant, K_m, and the maximal transport velocity, v_{max}. Thus we could determine the distributions of these transport parameters in the measured cell populations. The averages of K_m and v_{max} agreed very well with those deter-

Received for publication 16 December 1994 and in final form 13 April 1995.

Address reprint requests to Dr. Reiner Peters, Institut für Medizinische Physik und Biophysik, Westfälische Wilhelms-Universität, Robert-Koch-Strasse 31, 48149 Münster, Germany. Tel.: 011-49-251-83-6933; Fax: 011-49-251-83-5121; E-mail: petersr@uni-muenster.de.

0006-3495/95/07/30/12 $2.00

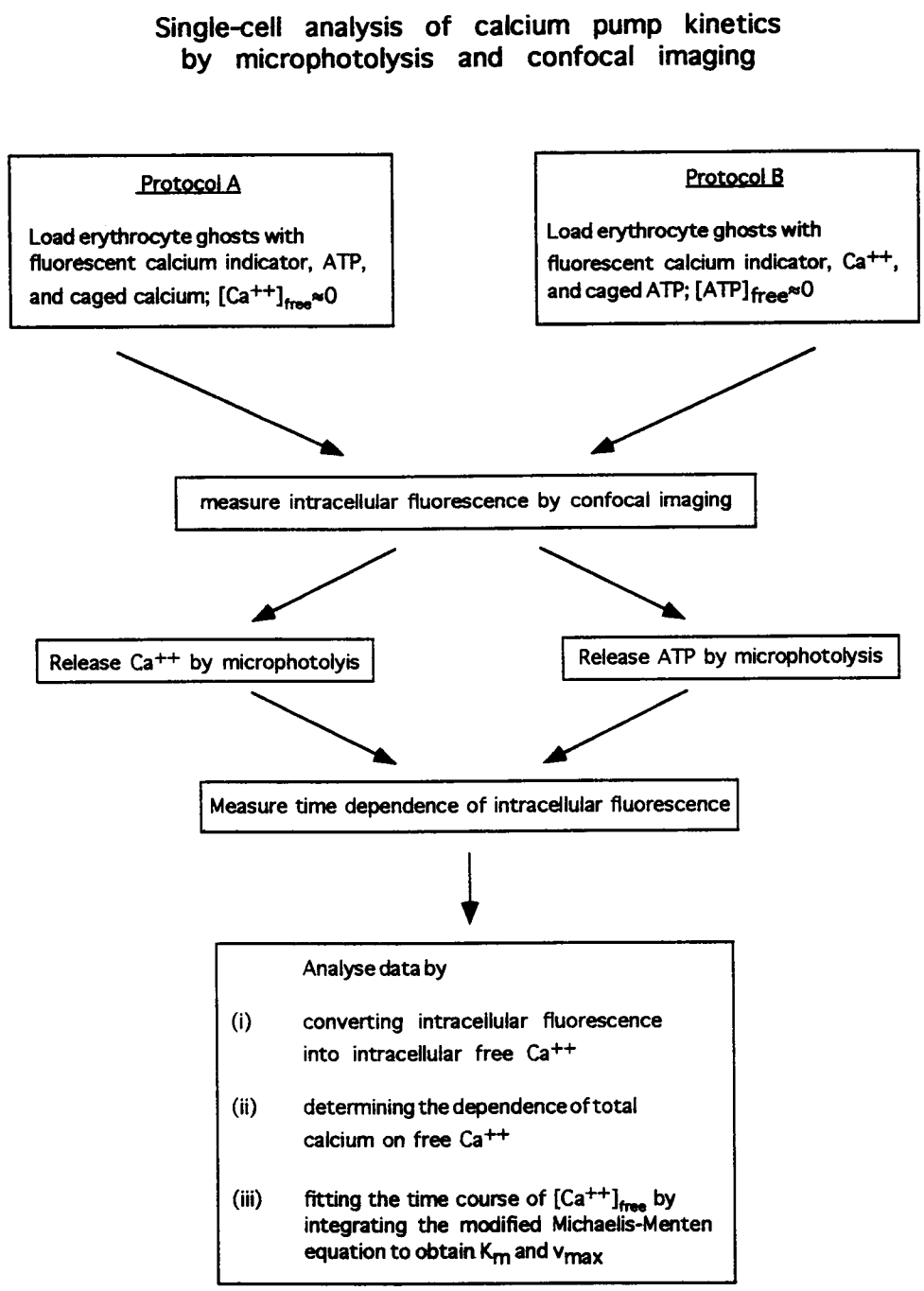

FIGURE 1 Experimental strategies for single-cell analysis of calcium pump kinetics. Human erythrocyte ghosts were loaded with a fluorescent calcium ion indicator and either caged calcium and ATP (protocol A) or calcium and caged ATP (protocol B). The calcium pump was then activated by photolytic release of calcium or ATP and the time course of intracellular fluorescence was followed by confocal imaging, as described in the text.

mined previously by macroscopic measurements (Garrahan and Rega, 1990; James-Kracke, 1992).

Although the method was originally developed with erythrocyte ghosts, it has the potential for general application to eukaryotic cells. This possibility may be particularly relevant for studies in which site-directed mutagenesis together with transient expression in eukaryotic cells is used to analyze structure-function relationships in the PMCA. Furthermore, the method may be used to study any ATP-dependent membrane pump with a transport substrate that can be visualized by a fluorescent indicator.

THEORY

Experimentally, human erythrocyte ghosts were loaded with a fluorescent calcium indicator and caged compounds according to Fig. 1. The PMCA was then activated by a sudden photolytic release of caged compounds at time $t = 0$ and the relative intracellular fluorescence intensity, $F(t)$, measured in individual erythrocyte ghosts as a function of time. The evaluation of the experimental data proceeded in two steps. First, $F(t)$ was converted into the intracellular concentration of free calcium ions, $[Ca^{2+}]_{free}(t)$. Second, $[Ca^{2+}]_{free}(t)$ was fitted by the integrated, slightly modified

Michaelis-Menten equation to obtain the kinetic parameters K_m and v_{max} of the PMCA. The Michaelis-Menten equation was modified such that the dependence of $[Ca^{2+}]_{free}(t)$ on $[Ca^{2+}]_{total}(t)$ could be taken into account.

Calculation of the free calcium ion concentration

The relative fluorescence intensity determined by confocal imaging inside individual ghosts was corrected for a low level of background fluorescence and a small degree of photobleaching induced by the scanning process, as described in Materials and Methods. From the corrected fluorescence intensities, $F(t)$, the absolute free calcium concentrations $[Ca^{2+}]_{free}(t)$ were calculated according to Tsien et al. (1982) by

$$[Ca^{2+}]_{free,i} = K_d \frac{F_{exp,i} - F_{min,i}}{F_{max,i} - F_{exp,i}}. \quad (1)$$

Here, K_d is the dissociation constant for calcium of the calcium indicator. K_d was experimentally determined for both Calcium Green 2 and Calcium Green 5N (Grynkiewiez et al., 1992) at the conditions used in this study, i.e., inside ghosts with the confocal laser scanning microscope (see Materials and Methods and Results). F_{max} is the maximal fluorescence intensity observed when the calcium indicator is saturated with calcium. For the conversion of $F(t)$ into $[Ca^{2+}]_{free}(t)$ according to Eq. 1, F_{max} and F_{min} were determined for each cell individually because the intracellular concentration of indicator dye varied slightly among ghosts (see Results). This is indicated by the subscript i in Eq. 1. In the case of ghosts loaded with the caged calcium compound DM-nitrophen (DMN) and an ATP-regenerating system, F_{max} was approximated by $F(t = 0)$, the intracellular fluorescence intensity measured immediately after the photolytic release of an excess of calcium ions. In the case of ghosts loaded with an excess of calcium ions and caged ATP, F_{max} was approximated by $F(t < 0)$, the intracellular fluorescence intensity before photolysis. F_{min} is the minimal fluorescence intensity, observed in the absence of calcium. For experiments with caged calcium, F_{min} was approximated by $F(t < 0)$, because in this case the free calcium concentration before photolysis is in the nanomolar range. For experiments with caged ATP, F_{min} was approximated by the fluorescence measured a long time after photolysis, $F(t \to \infty)$.

Great care was taken to verify that the quoted approximations, namely $F_{max} \approx F(t = 0)$ and $F_{min} \approx F(t < 0)$ (protocol A) or $F_{max} \approx F(t < 0)$ and $F_{min} \approx F(t \to \infty)$ (protocol B) were valid. Ghosts loaded with a calcium indicator, as in transport measurements, were made permeable for calcium ions by incubation with the ionophore A23187 and dispersed in a buffer containing either 1 mM Ca^{2+} or 100 μM EGTA, which saturates the calcium indicator or totally depletes it of calcium ions, respectively. The fluorescence intensities measured with these preparations, on average, were identical with the F_{max} and F_{min} values determined as described above.

Calculation of the relation between total and free calcium concentration

By Eq. 1, $[Ca^{2+}]_{free}(t)$ was derived from the experimentally determined fluorescence of the calcium indicator. However, to determine the characteristic parameters of the calcium pump, K_m and v_{max}, it was necessary (see Eq. 2 below) to know the total and free calcium concentrations. In the present experimental system it may be primarily ATP, DMN, the photolyzed form of DMN, and the calcium indicators that bind calcium. The situation is further complicated by the fact that Mg^{2+}, employed in high concentrations during hemolysis, competes with calcium for binding by the quoted substances. Taking into account the various washing steps during the preparation of the ghosts, the final Mg^{2+} concentration was estimated as approximately 10 μM. Other parameters such as calcium-binding proteins and calcium storage sites, which are present in living cells and there play a prominent role, were assumed to be negligible in erythrocyte ghosts.

Determination of the relationship between free and total calcium was required for the two different experimental protocols involving DMN or caged ATP. Unfortunately, explicit solutions of the corresponding coupled mass action equations were not available. Therefore, we utilized an iterative, rapidly converging computer program. The input parameters for the computer program were the total concentrations of the involved species and their equilibrium constants for calcium and magnesium binding. The concentrations of caged compounds and their photolyzed forms were calculated assuming a photolysis efficiency of 50% (see Materials and Methods). The dissociation constants value for DMN were taken from Kaplan and Ellis-Davies (1988) ($K_{d,Ca^{2+}}$ before photolysis = 5 nM, $K_{d,Mg^{2+}}$, before photolysis = 5 μM, $K_{d,Ca^{2+}}$ or $K_{d,Mg^{2+}}$ = 3 mM). Values for ATP were taken from Martell and Smith (1974) and corrected for ionic strength with the computer program CALCIUM (Föhr et al., 1993) resulting in $K_{d,Ca^{2+}} = 288$ μM and $K_{d,Mg^{2+}} = 174$ μM. Examples for the outcome of such calculations are shown in Fig. 2.

Determination of K_m and v_{max}

The kinetics of the calcium pump can be approximated (Garrahan and Rega, 1990) by the Michaelis-Menten equation:

$$\frac{d[Ca]_{total}}{dt} = -\frac{v_{max}[Ca^{2+}]_{free}}{K_m + [Ca^{2+}]_{free}} \quad (2)$$

Here we consider the amount of calcium transported per cell and hence deal with the total internal calcium concentration. K_m and v_{max} are the Michaelis-Menten constant and the

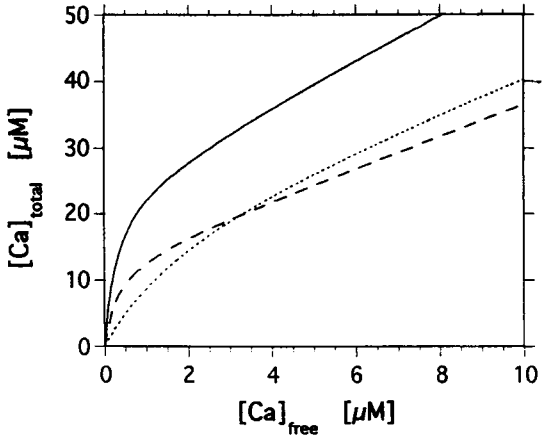

FIGURE 2 Functional relationship between total and free calcium concentrations within erythrocyte ghosts prepared according to protocol A or B (see Fig. 1). The curves were calculated by a rapidly converging iterative procedure based on the respective mass action equations. Calcium binding components were, respectively, 24 μM Calcium Green 2, 700 μM ATP (full line, corresponding to protocol B), 13 μM Calcium Green 2, 400 μM ATP, 100 μM photolyzed DMN (dashed line, corresponding to protocol A), 20 μM Calcium Green 5N, 400 μM ATP, and 100 μM photolyzed DMN (dotted line, corresponding to protocol A).

maximal transport rate per ghost in units of mol l^{-1} ghost^{-1} s^{-1}, respectively. Eq. 2 was rearranged to yield

$$\frac{d[Ca^{2+}]_{free}}{dt} = \frac{v_{max}[Ca^{2+}]_{free}}{(K_m + [Ca^{2+}]_{free})\dfrac{d[Ca]_{total}}{d[Ca^{2+}]_{free}}}. \quad (3)$$

By using the functional relationship between $[Ca]_{total}$ and $[Ca^{2+}]_{free}$ as given in Fig. 2, Eq. 3 was numerically integrated by a fifth order Runge-Kutta method yielding $[Ca^{2+}]_{free}$ as a function of time with K_m and v_{max} as parameters (Press et al., 1992). Finally, a Levenberg-Marquardt minimization routine was employed to search for the optimal values of K_m and v_{max} describing the individual data sets of single erythrocyte ghosts (Press et al., 1992).

MATERIALS AND METHODS

Reagents and solutions

Lysis solution contained 5 mM $MgSO_4$ and 0.4 mM acetic acid, pH 4.2. Transport buffer A consisted of 13 μM Calcium Green 2 or 25 μM Calcium Green 5N (Molecular Probes, Eugene, OR), 200 μM DMN, 400 μM glutathione, 1 mM ATP, 2.5 mM phosphocreatine, 500 U/l phosphocreatine kinase, 20 mM HEPES, 160 mM KCl, and 220 μM $CaCl_2$. Glutathione was added to trap nitrosoketone photoproduction (Kaplan et al., 1978). Taking into account the calcium buffer capacity (see above) of this solution and an estimated 50% efficiency of DMN photolysis, the $[Ca^{2+}]_{free}$ was estimated to be ≤100 nM before and approximately 30 μM after photolysis. Transport buffer B contained 13 μM Calcium Green 2, 1 mM caged ATP, 1 mM glutathione, 20 mM HEPES, 160 mM KCl, and 50 μM $CaCl_2$. Here, $[Ca^{2+}]_{free}$ was estimated to be approximately 15 μM. KCl buffer was composed of 160 mM KCl and 20 mM HEPES, pH 7.4. No measures were taken to control $[Ca^{2+}]_{free}$ in this buffer. It contained therefore an ubiquitous level of free Ca^{2+} of ~2–3 μM, as verified by measurements with an ion-sensitive electrode.

The calcium indicator dyes were dissolved in KCl buffer and routinely used at a final concentration of 10–25 μM. To determine their dissociation constants K_d for calcium, ghosts were prepared in KCl buffer and loaded with the calcium indicators. Ghosts were then permeabilized for Ca^{2+} by incubation with the ionophore A23187 (2 μM) and resuspended in H-EDTA buffers of defined calcium concentrations prepared according to Tsien (1989). The intracellular fluorescence intensity was measured in individual ghosts by confocal imaging as described below. The K_d was determined from the dependence of the intracellular fluorescence intensity on the Ca^{2+} concentration.

The caged ATP adenosine-5′-triphosphate, P^3-1-(2-nitrophenyl)-ethyl ester (disodium salt) and the caged calcium compound DM-nitrophen (tetrasodium salt) were purchased from Calbiochem (San Diego, CA). Stock solutions were prepared in buffer and stored at −70°C.

Preparation of erythrocyte ghosts

Human erythrocyte ghosts were prepared according to two different protocols as indicated in Fig. 1. In both cases blood was drawn from healthy donors into citrate and used immediately. After separation of erythrocytes from white blood cells by centrifugation (2000 rpm for 10 min at 4°C), the erythrocytes were washed once with phosphate-buffered saline (pH 7.4) and twice with an isotonic NaCl solution (154 mM) at 4°C. Finally, the erythrocyte suspension was adjusted to a hematocrit of 50%. After carefully precooling all media and materials to 0°C, lysis was performed on ice. Erythrocytes (0.7 ml) were added to 30 ml of the lysis solution and incubated for 15 min with gentle stirring. Ghosts were then sedimented (16,000 × g for 20 min at 0°C), resuspended in 30 ml of KCl buffer, again sedimented, and finally resuspended in 1.75 ml of buffer. Then, 0.4 ml of this suspension was mixed with 0.1 ml of transport buffer A (protocol A) or B (protocol B) and incubated for 15 min on ice. Erythrocyte ghosts were resealed by incubation at 37°C for 45 min and stored on ice until use.

Measurement of intracellular fluorescence intensities by confocal microscopy

Before microscopic studies, erythrocyte ghosts were washed twice with KCl buffer containing 2–3 μM free Ca^{2+} (see above). Some experiments were performed in KCl buffer supplemented with 100 μM EGTA to completely remove free Ca^{2+} or in KCl buffer supplemented with $CaCl_2$ to raise the extracellular Ca^{2+} level to 20 μM or 2 mM. Transport inhibition studies were performed by adding 50 μM sodium vanadate or 20 μM $LaCl_3$ to the extracellular KCl buffer. The ghost suspension was then filled into microslides, i.e., flattened glass capillaries with inner dimensions of 0.05 mm × 1 mm × 30 mm. The microslides were allowed to rest for 20 min, during which time most of the erythrocyte ghosts adsorbed spontaneously to the lower internal glass surface. The microslide was then sealed at the ends with silicon paste and mounted upside down (i.e., with the layer of adsorbed ghosts on the upper side) on a glass slide.

A confocal laser scanning microscope (CLSM; Leica, Heidelberg, Germany) was employed to generate images of the ghosts. By means of the confocal aperture of the CLSM the effective thickness of the optical section was adjusted to ≤1 μm. A microslide with a layer of adsorbed ghosts was placed on the stage of the CLSM and, with a 40-fold oil-immersion objective lens of 1.3 numerical aperture, focused such that the focal plane coincided with the center of the ghost layer. With a zoom factor of 2, the size of the imaged area amounted to 62.5 × 62.5 μm^2. The fluorescence of the calcium indicators was excited by the 488-nm line of an argon laser, thus avoiding photolysis of the caged compounds that exhibit absorption maxima at 360 nm. The degree of calcium indicator photobleaching by imaging was determined by generating image series of ghosts prepared without caged components or according to protocol B, but without photolyzing the caged ATP. The intracellular fluorescence intensities of indi-

vidual ghosts in these image series were determined as a function of image number. The laser beam power was reduced to a degree at which the reduction of intracellular fluorescence was <2% per image. The image series used for quantitative studies of the PMCA kinetics were corrected for this degree of photobleaching. Care was taken to adjust the offset and the photomultiplier voltage in such a way that the measured signal was linearly related to the fluorescence intensity and that the dynamic range of the instrument (256 grey levels) was utilized.

The DMN or the caged ATP enclosed in the ghosts was photolyzed by irradiating the specimen on the stage of the CLSM through the vertical illuminator. A 100-W high pressure mercury lamp was used as a light source isolating the 366-nm line by appropriate filters. The field diaphragm of the vertical illuminator was adjusted such that irradiated and imaged areas were approximately coincident. A photo shutter was integrated into the irradiation pathway to determine the irradiation time. By measuring the effect of irradiation time on the increase of intracellular fluorescence (in case of DMN photolysis, protocol A of Fig. 1) or initial pumping activity (in case of caged ATP photolysis, protocol B of Fig. 1), we very roughly estimated that an irradiation time of 0.25 s was required to decompose ~50% of the caged compounds. Therefore, in all of the experiments, an irradiation time of 0.25 s was employed.

A transport measurement consisted of: i) acquisition of a confocal fluorescence image of a specimen area before photolysis (prebleach image), ii) release of Ca^{2+} (protocol A) or ATP (protocol B) by a 0.25-s UV irradiation, and iii) acquisition of 5–15 images at various times after photolysis (monitor images). To evaluate the images in terms of the time-dependent relative intracellular fluorescence intensities we created a special computer software module. The module allowed an arbitrary number of work windows to be placed in the image by using the trackball of the microscope workstation. The work windows were adjusted to have a size of 2.45 μm × 2.45 μm and placed in the centers of individual ghosts. Thus, the relative fluorescence intensity originating from an intracellular volume of ~6 fl (2.45 μm × 2.45 μm × 1.0 μm) was obtained cell by cell. For analysis of a complete time series of images it was necessary to set the work windows only once. The program would then automatically scan through the image stack extracting the time dependent fluorescence data.

RESULTS

Dissociation constant of the fluorescent calcium indicator Calcium Green

In the present study the fluorescent calcium indicator Calcium Green 2 and Calcium Green 5N were employed. Because K_d values may depend sensitively on a variety of parameters such as ionic strength, exact ion composition, and pH value we measured the respective K_d values at our experimental conditions. For this purpose, erythrocyte ghosts were prepared exactly as in transport measurements, made permeable for Ca^{2+} by the ionophore A23187, and dispersed in calcium buffers with defined free Ca^{2+} concentrations. Then, the intracellular fluorescence intensity was measured by confocal imaging in dependence of the free Ca^{2+} concentration. The experimental data were fitted by Eq. 1 yielding a K_d of 0.3 ± 0.05 μM and of 2.0 ± 0.3 μM (mean ± SD) for Calcium Green 2 and Calcium Green 5N, respectively. Furthermore, we checked that the K_d values were not significantly changed by DMN or caged ATP at concentrations used in transport measurements (Zucker, 1992).

Imaging of the fluorescence intensity inside single ghosts

The method described in this paper depends on the capability of confocal imaging to generate thin optical sections and to reject out-of-focus fluorescence. This permits one to selectively monitor the fluorescence originating from a thin

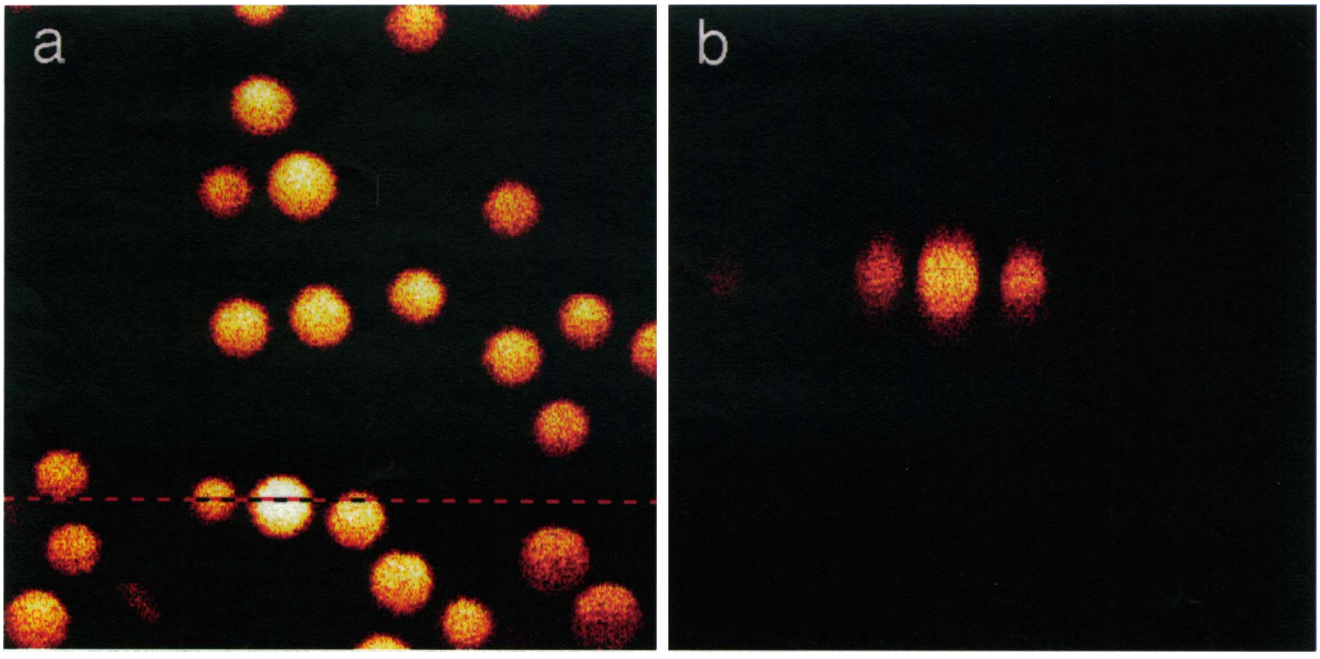

FIGURE 3 Imaging of the intracellular fluorescence in erythrocyte ghosts by confocal microscopy. Ghosts were prepared according to protocol B (Fig. 1). A total area of 50 × 50 μm^2 was imaged. (*a*) Optical section parallel to the glass capillary surface (*xy* plane, eightfold line scan). (*b*) Optical section perpendicular to the glass surface along the dashed line indicated in *a* (*xz* plane).

fluid layer inside a ghost and thus to obtain a relative measure of the intracellular fluorescence intensity directly related to $[Ca^{2+}]_{free}(t)$. The actual resolution of the CLSM used in the present study was measured by using horizontal and vertical sections of ghosts (Fig. 3) prepared according to protocol B, i.e., loaded with Calcium Green 2, free Ca^{2+} in excess (approximately 20 μM), and caged ATP. These ghosts were fluorescent because the calcium indicator was completely saturated with Ca^{2+}. Fig. 3*a* shows an optical section (50 × 50 μm^2) parallel to the surface of the glass capillary approximately 2–3 μm below the glass-buffer interface. Fig. 3*b* shows a corresponding *xz*-section of the specimen acquired along the dashed line in Fig. 3*a*. The slight elliptical elongation of the ghosts in Fig. 3*b* is a result of lower resolution in the axial direction and spherical aberration at the glass-liquid interface. Under the imaging conditions employed for the experiments we estimated the resolution to be approximately <0.3 μm in the radial and <0.8 μm in the axial direction.

Fig. 3 also shows that the intracellular fluorescence varied substantially among ghosts. A similar degree of variation was observed in all experiments, independent of the protocol. It also occurred in A23187-permeabilized ghosts suspended in calcium buffers of defined Ca^{2+} concentrations. We concluded that the variation was a result of different intracellular concentrations of the calcium indicator, suggesting that the permeabilization of the erythrocyte membrane by hypotonic hemolysis and the uptake of highly charged substances from the medium into permeabilized ghosts was surprisingly heterogeneous, even for relatively small molecules such as calcium indicators.

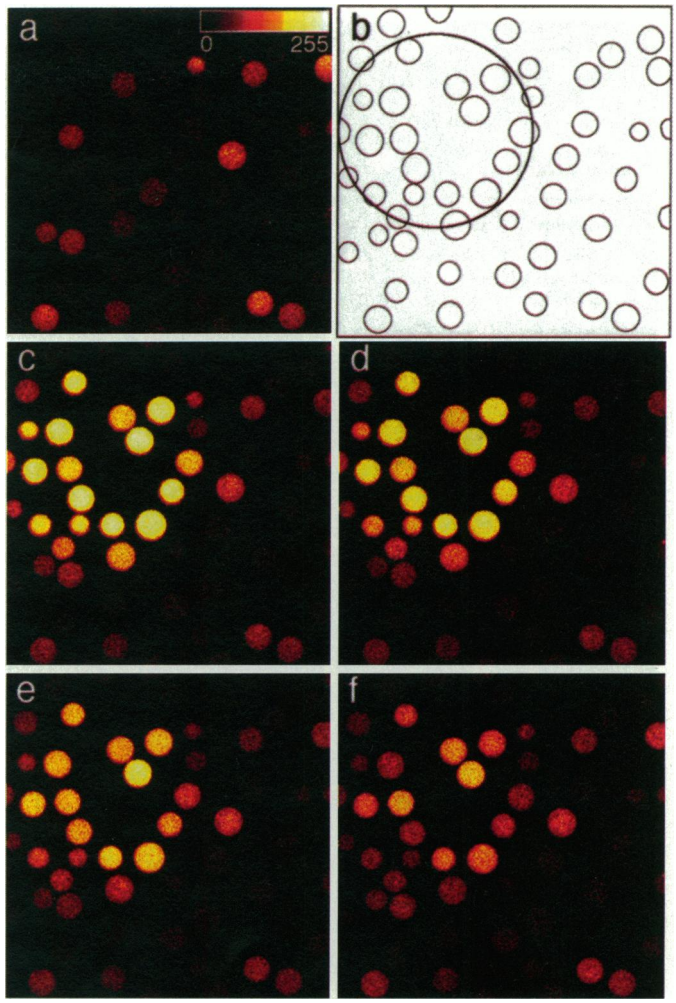

FIGURE 4 Visualization of calcium pump activity by confocal imaging according to protocol A (16 line scans averaged, imaged area = 62 × 62 μm^2). Erythrocyte ghosts were pepared according to protocol A and contained 13 μM Calcium Green 2, 220 μM DMN, 200 μM calcium, 400 μM glutathione, 400 μM ATP, 2.5 mM phosphocreatine, 2 U/ml phosphocreatine kinase, 20 mM HEPES, and 160 mM KCl (final concentrations). (*a*) Before photolysis. (*b*) Outlines of all ghosts that were visible on the computer screen (small circles) and of the photolysis area (large circle). (*c-f*) 0, 180, 360, and 600 s after photolysis, respectively.

Visualization of the calcium pump activity

A typical example for an experiment according to protocol A is shown in Fig. 4. Ghosts were loaded with Calcium Green 2, DMN, ATP, and an ATP-regenerating system. Before photolysis (Fig. 4*a*), the intracellular concentration of free Ca^{2+} was quite low (<100 nM). Accordingly, the intracellular fluorescence was minimal. The positions of all ghosts that were clearly recognizable on the computer screen and of the photolysis field are indicated in Fig. 4*b*.

Photolysis of DMN was expected to raise the intracellular concentration of free Ca^{2+} to approximately 30 μM, thereby totally saturating the calcium indicator. In fact, photolysis strongly increased the intracellular fluorescence (Fig. 4*c*). In contrast, the fluorescence of ghosts outside the photolysis field and thus not exposed to UV light remained virtually unaffected (Fig. 4*c*).

The action of the PMCA can be directly observed in Fig. 4, *c-f*, taken at t = 0, 180, 360, and 600 s after photolysis, respectively. The intracellular fluorescence of ghosts within the photolysis field is seen to decrease with time, indicating that the intracellular $[Ca^{2+}]_{free}$ was strongly reduced. This occurred in spite of the fact that the extracellular $[Ca^{2+}]_{free}$ amounted to 2–3 μM (see Materials and Methods). These results provided strong evidence that Ca^{2+} export from the ghosts was not a passive process based, for instance, on a leakiness of the erythrocyte membrane.

The entire process comprising photolysis, sudden fluorescence increase, and time-dependent fluorescence decrease could be repeated with the same sample (data not shown), suggesting that neither the photolysis by UV light nor the imaging process involving illumination with the 488-nm laser line inactivated the pump.

An example for an experiment according to protocol B is shown in Fig. 5. Here ghosts were loaded with Calcium Green 2, free Ca^{2+} in excess (approximately 10 μM), and caged ATP. Under these conditions the calcium indicator was already saturated at the beginning of the experiment giving rise to a high intracellular fluorescence (Fig. 5*a*). The

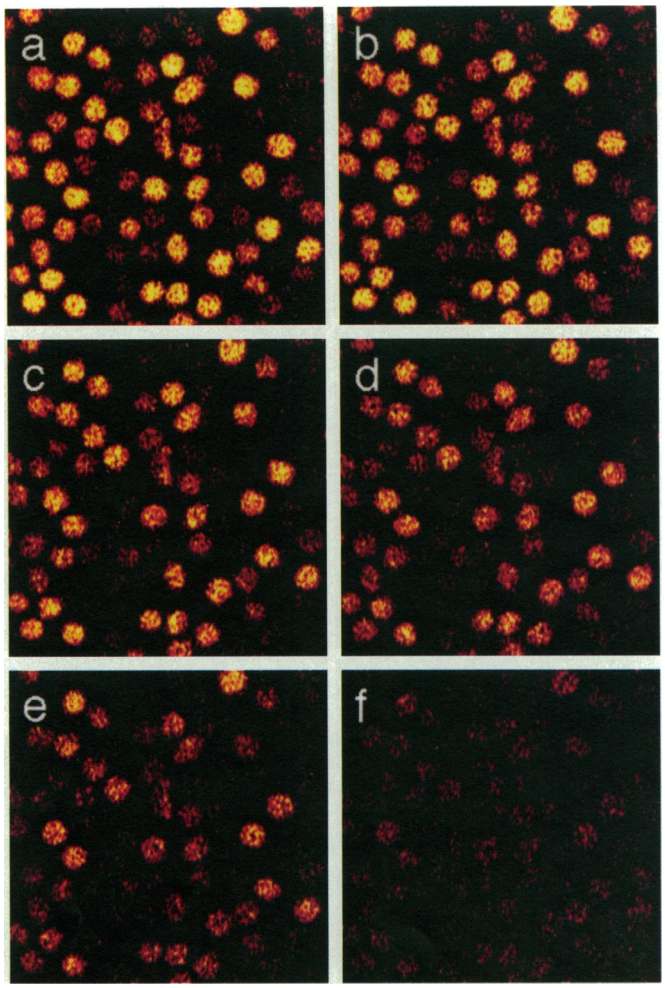

FIGURE 5 Visualization of calcium pump activity by confocal imaging according to protocol B (single line scan, imaged area = 80 × 80 μm^2). Ghosts were pepared according to protocol B and contained 1 mM caged ATP, 12 μM Calcium Green 2, 50 μM calcium, 1 mM glutathione, 20 mM HEPES, and 160 mM KCl (final concentrations). (*a*) Before photolysis. (*b-f*) 5, 30, 50, 70, and 200 s after photolysis, respectively.

PMCA was activated by photolytic release of ATP, its action observable by a rapid decrease of intracellular fluorescence (Fig. 5). The images shown were recorded at t = 5, 30, 50, 70, and 200 s (Fig. 5, *b-f*, respectively) after the photolysis. Eventually (Fig. 5*f*), the intracellular fluorescence decreased to almost background level, despite an extracellular $[Ca^{2+}]_{free}$ of approximately 2–3 μM. This demonstrated once again that Ca^{2+} export was an active process.

Independence of Ca^{2+} pumping on the extracellular Ca^{2+} concentration and inhibition by vanadate and lantanate

Some of the well known characteristics of the PMCA are its ability to transport Ca^{2+} against large concentration gradients and its inhibition by orthovanadate and La^{3+} ions (Carafoli, 1991). To determine whether these features would be faithfully reproduced by our experimental system, confocal images were evaluated for intracellular fluorescence intensities of individual ghosts. These intensity values were averaged and plotted versus time after photolysis for a variety of experimental conditions. Fig. 6*a* shows the results of experiments according to protocol A at different extracellular Ca^{2+} concentrations or in the presence of 50 μM vanadate. Fig. 6*b* shows the results of experiments with

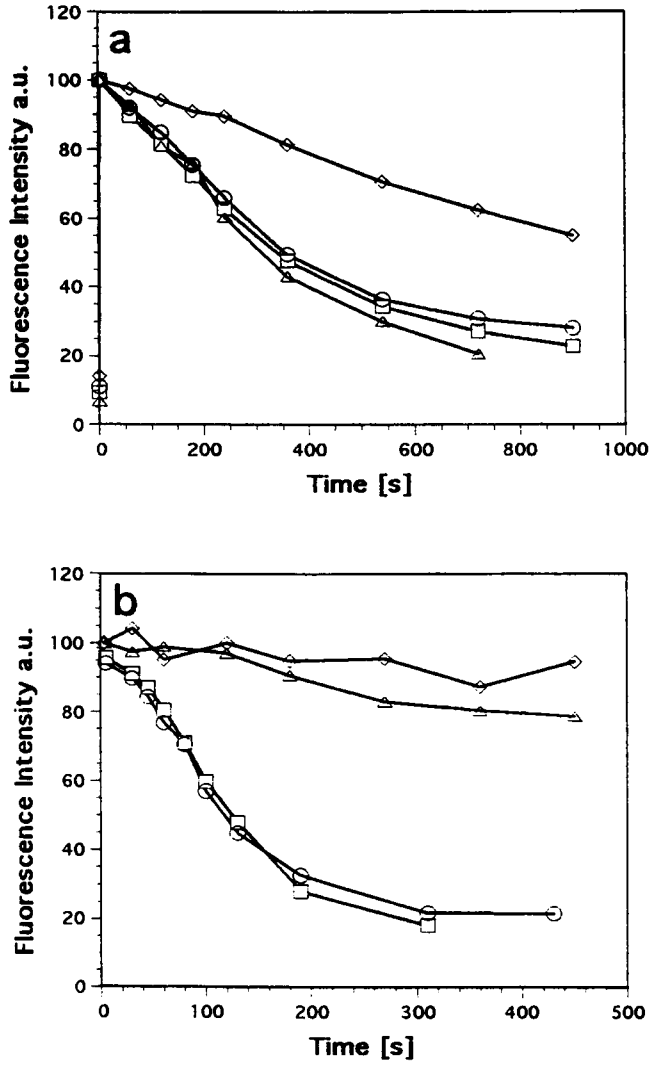

FIGURE 6 Independence of Ca^{2+} pumping on the extracellular Ca^{2+} concentration and inhibition by vanadate and lantanate. The intracellular fluorescence of individual ghosts, prepared and treated according to protocol A (*a*) or B (*b*), was averaged and plotted versus time after photolyis. (*a*) Cells were loaded with 100 μM DMN, 100 μM Ca^{2+}, and 10 μM Calcium Green 2 and immersed in media of varying composition (□, 100 μM EGTA corresponding to 0 μM Ca^{2+}; ○, 20 μM Ca^{2+}; △, 2 mM Ca^{2+}; ◇, 50 μM vanadate).(*b*) Cells were loaded with 1 mM caged ATP, 40 μM Ca^{2+}, and 12 μM Calcium Green 2 and immersed in media with increasing Ca^{2+} concentrations (□, 100 μM EGTA; ○, 2 mM Ca^{2+}), with 50 μM vanadate (△), or with 20 μM La^{3+} (◇). In the experiments according to both protocols, the rate of the extrusion process was independent of the extracellular Ca^{2+} concentrations up to millimolar concentrations. In addition, the presence of vanadate largely inhibited the efflux, and La^{3+} blocked it completely. These data provide evidence that the calcium efflux is indeed a result of the action of the PMCA.

caged ATP according to protocol B with increasing extracellular Ca^{2+} concentrations or in the presence of 50 μM vanadate or 20 μM La^{3+}. In all of these experiments the rate of Ca^{2+} transport was virtually independent of the extracellular Ca^{2+} concentration, even when in the millimolar range. Ca^{2+} transport was largely inhibited by vanadate and completely blocked by La^{3+}. Inhibition of the PMCA by vanadate is known to be enhanced by Mg^{2+} but reduced by high concentrations of Ca^{2+} and ATP (Barrabin et al., 1980). Because in our system the Mg^{2+} concentration was low and the Ca^{2+} and ATP concentrations were high a complete inhibition was not expected.

Quantification of the calcium pump activity

The first step of calcium pumping quantification consisted of plotting the intracellular fluorescence intensities of individual ghosts versus time after release of either Ca^{2+} (protocol A, Fig. 7*a*) or ATP (protocol B, Fig. 7*b*). In both cases the time course of fluorescence had a sigmoid shape. This essentially reflected the nonlinear dependence of the calcium indicator fluorescence on the free Ca^{2+} concentration. Fluorescence changes are largest if the free Ca^{2+} concentrations are in the range of the K_d of the calcium indicator. However, if the free Ca^{2+} concentrations are an order of magnitude above or below the K_d, concentration changes yield only small fluorescence changes that are difficult to detect.

A single-cell analysis as shown in Fig. 7 permits, in general, detection of subpopulations in heterogeneous samples. In the present case the PMCA was studied in erythrocyte membranes derived from healthy donors; therefore subpopulations of ghosts with different PMCA activities were not expected. Fig. 7*a* reveals, however, that a minor fraction of ghosts showed no or little fluorescence changes upon release of Ca^{2+}. Clearly, these were leaky ghosts that were not properly resealed during preparation or were damaged when the specimen was prepared.

The second step of calcium pumping quantification is demonstrated in Figs. 8 and 9. Fig. 8 pertains to experiments with caged calcium (protocol A) and gives data sets obtained with Calcium Green 2 or Calcium Green 5N, respectively. It may be noted that, because of its significantly higher calcium affinity, Calcium Green 2 remained saturated much longer than Calcium Green 5N. Immediately after photolysis, small fluctuations in signal intensity resulted in arbitrary, erroneous changes in the calculated free calcium concentration. Approximately 500 s were necessary before the free calcium concentration approached the K_d value of the indicator dye resulting in a marked decrease in fluorescence. Hence, for the numerical analyis we considered only calcium concentrations ranging between 5 and 0.2 K_d. Intracellular fluorescence (Figs. 8*a* and 9*a*) was first converted into free Ca^{2+} concentration by using Eq. 1 (circles and squares in Figs. 8*b* and 9*b*). The $[Ca^{2+}]_{free}(t)$ was then fitted by the integrated Michaelis-Menten equation

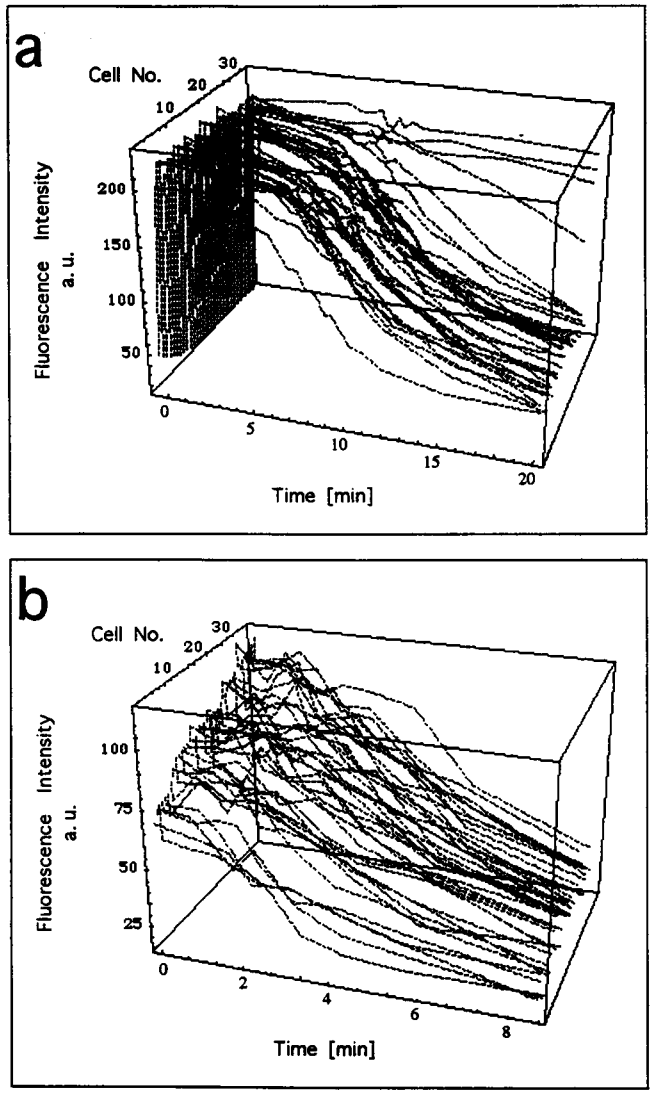

FIGURE 7 Time dependence of intracellular fluorescence in individual ghosts, prepared and treated according to protocol A (*a*) or B (*b*). (*a*) Photolyis at time $t = 0$ of cells loaded with caged calcium induced a strong increase in fluorescence as a result of the calcium release. The fluorescence intensity remained constant immediately after the photolysis despite a presumably strong activity of the calcium pump, because of the initial saturation of the calcium dye. Only when the free calcium concentration approached the K_d value of Calcium Green did the reduction in calcium become visible. A few ghosts exhibited high fluorescence intensity values before and after the photolysis (cell numbers 27–30), presumably as a result of cell damage. (*b*) Cells loaded with caged ATP exhibited initially a strong Calcium Green 2 fluorescence as a result of a saturating calcium concentration at the beginning of the experiment. The observed decrease in fluorescence was a result of the calcium extrusion after activation of the calcium pump by liberation of the ATP. Note the different time scales.

according to Eqs. 2 and 3 (dashed lines in Figs. 8*b* and 9*b*) taking the relationship between total and free calcium concentration (Fig. 2) into account.

The final step of the data analysis is presented in Figs. 10 and 11. For ghosts prepared according to protocol A, K_m was found to be 24 ± 14 μM, and v_{max} to be 1.0 ± 0.6 μM/(ghost s) (Fig. 10). No significant difference in the transport parameters could be detected for preparations with

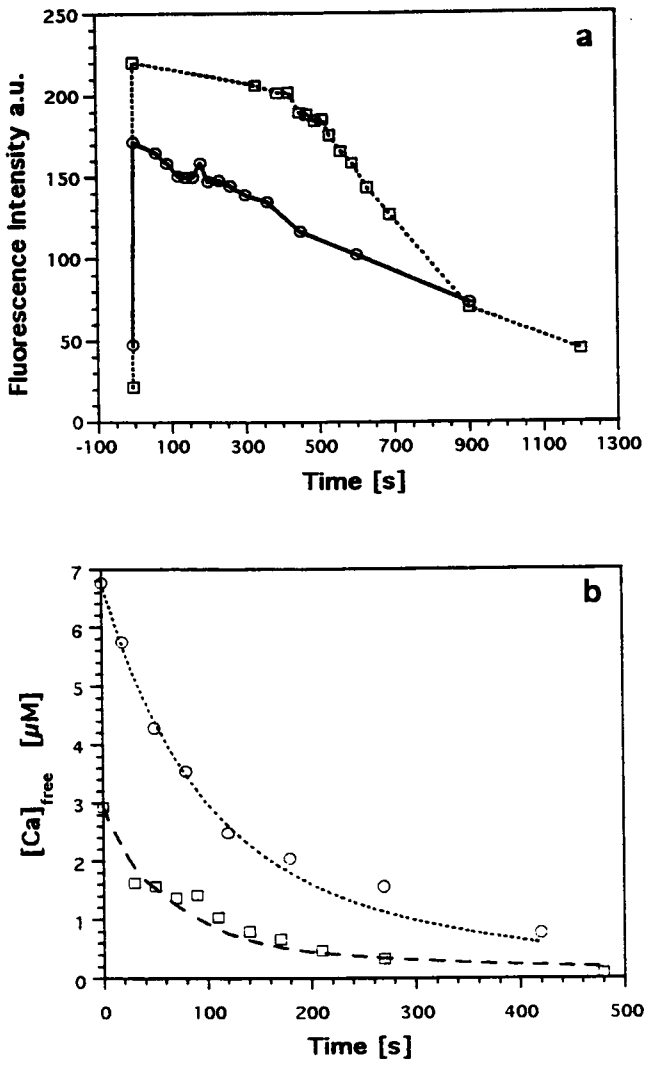

FIGURE 8 Conversion of intracellular fluorescence into free calcium concentration in experiments according to protocol A. (*a*) The time-dependent fluorescence of two individual ghosts, loaded either with Calcium Green 2 (□) or Calcium Green 5N (○), is shown before and after photolysis of caged calcium. (*b*) With the data shown in *a* the free calcium concentrations were calculated according to Eq. 1. The dashed and dotted lines give the result of the fitting process. For this purpose a modified Michaelis-Menten differential equation (Eq. 3) was numerically integrated, and the transport parameters v_{max} and K_m were determined by minimization of the χ^2 function by a Levenberg-Marquardt routine.

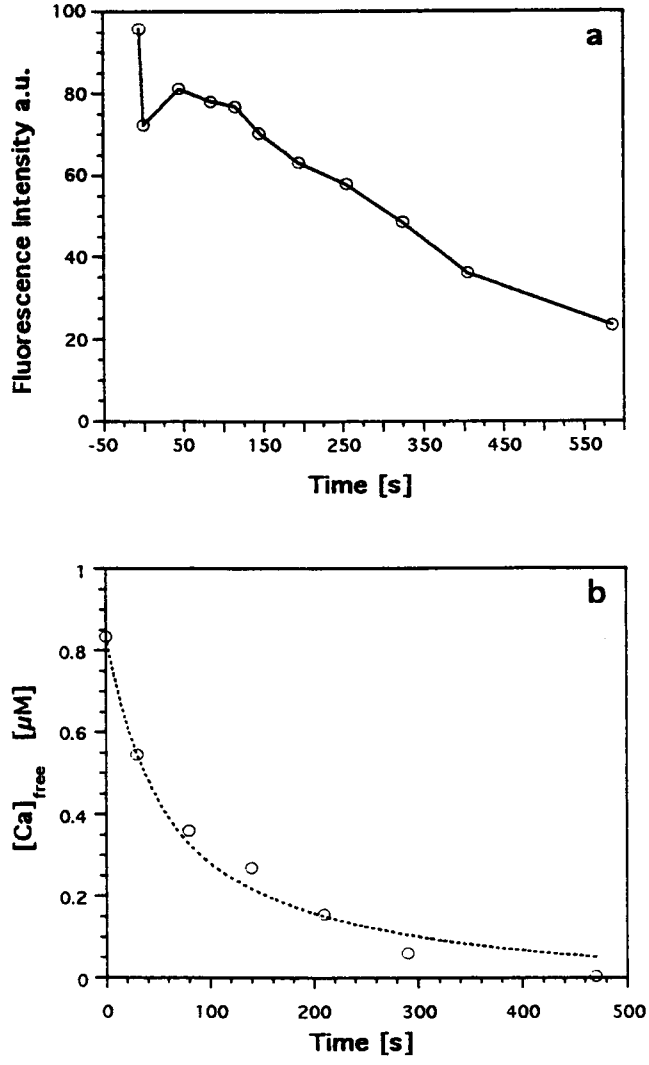

FIGURE 9 Conversion of intracellular fluorescence into free calcium concentration in experiments according to protocol B. (*a*) The time-dependent fluorescence of an individual ghost, loaded with Calcium Green 2, is shown before and after photolysis of caged calcium. (*b*) With the data shown in *a* the free calcium concentrations were calculated according to Eq. 1., the dotted line being the result of the fitting process performed as described in Fig. 8*b*.

Calcium Green 2 or Calcium Green 5N as ion indicator. The corresponding transport parameters for ghosts prepared according to protocol B were $K_m = 4 \pm 3$ μM and $v_{max} = 1.0 \pm 0.6$ μM/(ghost s) (Fig. 11).

DISCUSSION

In the present study a method for analyzing the activity of ion pumps in single cells has been developed. This method was used to measure the kinetics of the PMCA in individual erythrocyte ghosts. This was done by loading ghosts with a fluorescent calcium indicator and either caged calcium (protocol A) or caged ATP (protocol B). The PMCA was then activated by a short pulse of UV light, delivered to the ghosts in a confocal microscope, which induced the sudden release of either calcium or ATP. The fact that the calcium extrusion was unaffected by extracellular calcium concentrations of up to 1 mM, and that it could be inhibited by vanadate and La^{3+}, provided evidence that the observed efflux was mediated by the PMCA. The intracellular concentration of free calcium ions was monitored before and after microphotolysis by repetitive confocal imaging and analyzed by a mathematical model derived from the Michaelis-Menten equation. For ghosts prepared according to protocol A, the Michaelis-Menten constant K_m was found to be 24 ± 14 μM and the maximal transport rate v_{max} to be 1.0 ± 0.6 μM/(ghost s). The corresponding values for ghosts prepared according to protocol B were $K_m = 4 \pm 3$ μM and $v_{max} = 1.0 \pm 0.6$ μM/(ghost s).

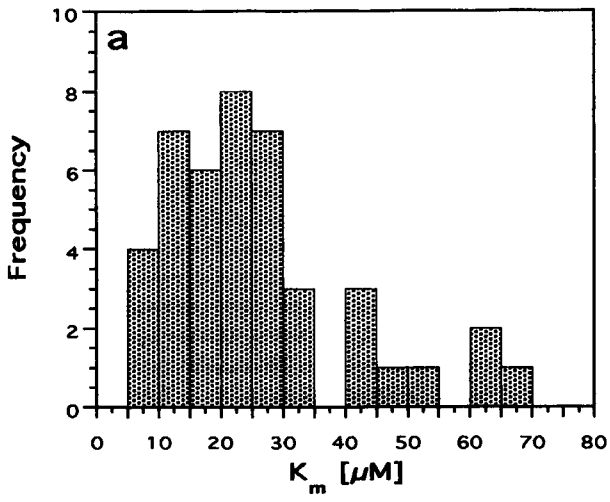

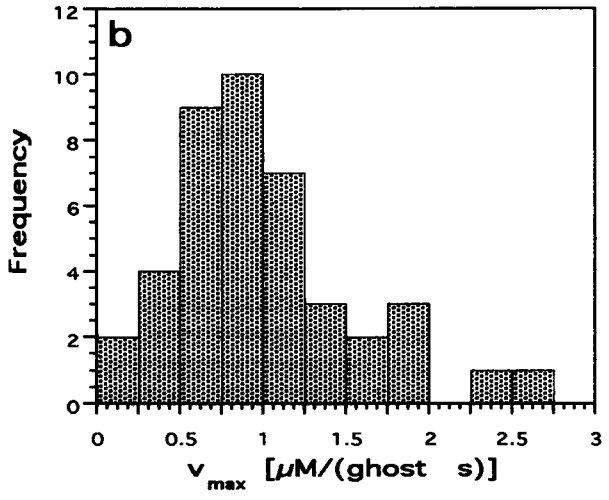

FIGURE 10 Single-cell distribution of the characteristic transport parameters determined according to protocol A. The distribution of the Michaelis-Menten constant K_m (*a*) and the maximal transport velocity v_{max} (*b*) are shown as derived from measurements on 43 individual ghosts of a particular ghost preparation.

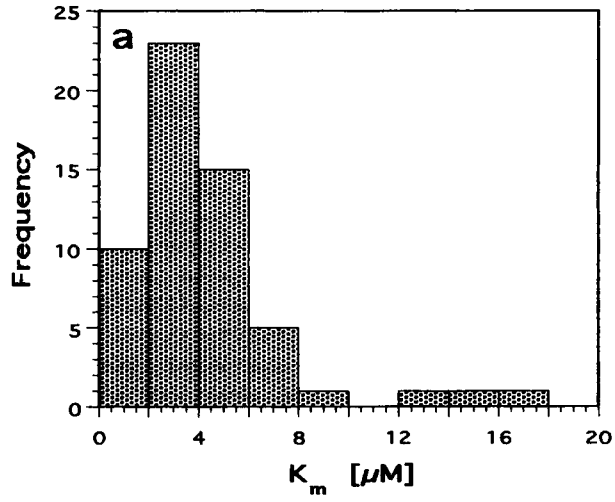

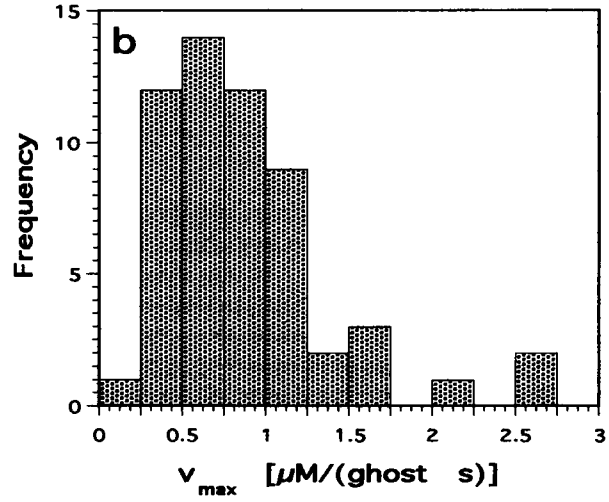

FIGURE 11 Single-cell distribution of the characteristic transport parameters determined according to protocol B. The distribution of the Michaelis-Menten constant K_m (*a*) and the maximal transport velocity v_{max} (*b*) are shown as derived from measurements on 57 individual ghosts of a particular ghost preparation.

That experiments with protocol A or B yielded quite different Michaelis-Menten constants may appear surprising at first glance. A closer look reveals, however, that the protocols actually differed with regard to one important aspect: before photolysis, free calcium was in the nanomolar range for protocol A but in the micromolar range for protocol B. The low calcium concentration level of protocol A caused the depletion of calmodulin from calcium, the dissociation of calmodulin from the PMCA, and the reduction of the PMCA activity to a basal level. Upon photolysis of DMN, according to protocol A, the concentration of free calcium, in principle, became sufficiently high to reactivate calmodulin and the PMCA. However, this process is well known (Scharff and Foder, 1978) as rather slow (10–20 min) and furthermore yields only a partial reactivation of the PMCA. Hence, experiments with protocol A essentially measured the basal activity of the PMCA (although the PMCA might have become activated during the course of the measurements). In contrast, in experiments with protocol B the PMCA was fully activated from the beginning. These conclusions were supported by experiments in which protocol B was used with ghosts that had been depleted in advance of calmodulin by lysis and repeated washing in the presence of 1 mM EGTA. Under these conditions the activity of the PMCA was found to be much smaller than in experiments with ghosts prepared as usual in the absence of EDTA (data not shown). With these preliminaries, the experimentally determined values of the Michaelis-Menten constant agree very well with published values determined by macroscopic measurements. For example, Garrahan and Rega (1990) list K_m values of 24.5 and 3.2 μM for the PMCA of the human erythrocyte membrane in the absence and presence of calmodulin, respectively.

Our value for v_{max} amounted to 1 ± 0.6 μM/(ghost s), independent of the experimental protocol applied. Our v_{max} value pertains to a single ghost. Thus, to compare our value

with literature values the volume of the erythrocyte ghost, V_{ghost}, must be taken into account. This was determined from confocal images as shown in Fig. 3 to be approximately V_{ghost} = 65 fl. Hence, the maximal pumping rate amounted to $v_{max} \times V_{ghost} \times N_L$ = 39,000 calcium ions/(ghost s), where N_L is Avogadro's number. Assuming that the PMCA occurs in 400–7200 copies per human erythrocyte ghost (Carafoli, 1991) the maximal pumping rate per single PMCA molecule then amounted to 5–100 calcium ions per second, a range that coincides exactly with values derived from macroscopic measurements. Garrahan and Rega (1990), for instance, quote a maximal pumping rate of ~50 calcium ions per second per active PMCA monomer.

The new method has the potential for extension to the study of PMCA mutants expressed transiently in intact eukaryotic cells. This is a major goal because the combination of molecular genetic techniques with functional measurements is a powerful approach for elucidating structure-function relationships in membrane transport proteins. In this regard the SERCA serves as a paradigm. A battery of mutants of the SERCA (Maruyama and MacLennan, 1988; reviewed by MacLennan et al., 1992) were created by gene technology and expressed transiently in COS-1 cells. The microsomal fraction of these cells provided a convenient system for analyzing functional properties of SERCA mutants such as ATP hydrolysis, calcium affinity, and transmembrane calcium transport. The same approach has been applied to the PMCA, although with less success. A method was established to transiently overexpress the PMCA and PMCA mutants in COS-1 cells (Adamo et al., 1992). However, transport measurements with crude plasma membrane fractions of PMCA-transfected cells containing presumably resealed inside-out plasma membrane vesicles showed only a moderate increase in calcium pumping activity compared with control samples. This was attributed to retention of the majority of the transiently expressed protein in the endoplasmic reticulum, which never reached the plasma membrane (Adamo et al., 1992). In fact, microsomal preparations of transfected cells showed largely enhanced PMCA activity (Enyedi et al., 1993) and could be successfully employed to study molecular parameters determining the regulation of the PMCA by calmodulin (Enyedi et al., 1993, 1994; Verma et al., 1994). The limited usefulness of plasma membrane fractions of transfected cells in functional studies of the PMCA (Adamo et al., 1992) may be caused by several factors in addition to the previously mentioned poor targeting of overexpressed PMCA from the endoplasmic reticulum to the plasma membrane. First, the transient expression in eukaryotic cells is frequently very heterogeneous; therefore, membrane fractions may be derived from cell populations in which many cells express little or no PMCA and only a few cells express large amounts. Second, only a fraction of the plasma membrane may form inside-out vesicles. Finally, only a fraction of the inside-out vesicles may reseal. All of these difficulties could be overcome by a method permitting measurement of the activity of the PMCA in single intact cells.

However, to extend the present method to intact eukaryotic cells several methodological amendments are required. First, cells should be loaded with the calcium indicator by simple incubation, with membrane-permeable acetoxymethyl esters that are available for both Calcium Green 2 and Calcium Green 5N. In addition, an acetoxymethyl ester derivative should be employed to load cells with caged calcium. A promising new caged calcium, nitrophenyl-EGTA, has been described recently (Ellis-Davies and Kaplan, 1994) and is now commercially available. Most important would be the discrimination between intracellular and plasma membrane-localized calcium pumps. Here, the high spatial resolution of confocal imaging should be of great value, and the major calcium storage sites such as the endoplasmic reticulum can probably be directly visualized. The intracellular calcium stores may be saturated by a first photolytic release of calcium and the activity of the PMCA measured after a second calcium release. In addition, the tumor promoter thapsigargin, which inhibits SERCA-type but not PMCA-type calcium pumps, may be employed. With regard to a potential functional analysis of mutant, transiently expressed PMCA forms it will be essential to quantitate the amount of plasma membrane-localized PMCA per cell, at least on a relative scale. This should be possible by the application of antibodies directed against extracellularly exposed epitopes of the PMCA.

It should be mentioned here that the determination of intracellular free calcium ion concentrations by application of fluorescent calcium indicators has been frequently discussed (reviewed in Morgan, 1993). One problem arises from the fact that the K_d value, i.e., the dissociation constant of the calcium indicator for calcium, which is required for converting fluorescence intensity into absolute calcium ion concentration, may strongly depend on the ionic and macromolecular composition of the medium. This is usually not known in intracellular applications. However, in the case discussed here this may not be crucial. An error in the K_d value would influence the parameters K_m and v_{max}, used to characterize PMCA activity, of all mutant PMCA forms in an identical manner, without obscuring relative differences.

This study was supported by the Deutsche Forschungsgemeinschaft (grant Pe 138/12).

REFERENCES

Adamo, H. P., A. K. Verma, M. A. Sanders, R. Heim, J. L. Salisbury, E. D. Wieben, and J. T. Penniston. 1992. Overexpression of the erythrocyte plasma membrane Ca^{2+} pump in COS-1 cells. *Biochem. J.* 285: 791–797.

Barrabin, H., P. J. Garrahan, and A. F. Rega. 1980. Vanadate inhibition of the Ca2+-ATPase from human red cell membranes. *Biochim. Biophys. Acta.* 600:796–804.

Becker, E. W. 1994. Biochemical model of the P-type ion pumps of the cell. *Naturwissenschaften.* 81:21–27.

Bonventre, J. V. 1992. Cellular calcium transport systems. *In* Membrane Transport in Biology, Vol. 5. J. A. Schafer, H. H. Ussing, P. Kristensen, and G. H. Giebisch, editors. Springer-Verlag, Berlin. 262–316.

Carafoli, E. 1991. Calcium pump of the plasma membrane. *Physiol. Rev.* 71:129–153.

Carafoli, E. 1992. The Ca^{2+} pump of the plasma membrane. *J. Biol. Chem.* 267:2115–2118.

Ellis-Davies, G. C. R., and J. H. Kaplan. 1994. Nitrophenyl-EGTA, a photolabile chelator that selectively binds Ca^{2+} with high affinity and releases it rapidly upon photolysis. *Proc. Natl. Acad. Sci USA.* 91: 187–191.

Enyedi, A., A. K. Verma, A. G. Filoteo, and J. T. Penniston. 1993. A highly active 120-kDa truncated mutant of the plasma membrane Ca^{2+} pump. *J. Biol. Chem.* 268:10621–10626.

Föhr, K. J., W. Warchol, and M. Gratzl. 1993. Calculation and control of free divalent cations in solutions used for membrane fusion studies. *Methods Enzymol.* 221:149–157.

Garrahan, P. J., and A. F. Rega. 1990. Plasma membrane calcium pump. *In* Intracellular Calcium Regulation. F. Bronner, editor. Wiley-Liss, New York. 271–303.

Grynkiewiez, G., M. Poenie, and R. Y. Tsien. 1992. A new generation of Ca^{2+} indicators with greatly improved fluorescence properties. *J. Biol. Chem.* 260:3440–3450.

James-Kracke, M. R. 1992. Calmodulin activation of the Ca^{2+} pump revealed by fluorescent chelator dyes in human red blood cell ghosts. *J. Gen. Physiol.* 99:41–62.

Jencks, W. P. 1989. How does a calcium pump pump calcium? *J. Biol. Chem.* 254:18855–18858.

Jencks, W. P. 1992. On the mechanism of ATP-driven Ca^{2+} transport by the calcium ATPase of sarcoplasmic reticulum. *Ann. NY Acad. Sci.* 671:49–57.

Kaplan, J. H., and G. C. R. Ellis-Davies. 1988. Photolabile chelators for the rapid photorelease of divalent cations. *Proc. Natl. Acad. Sci. USA.* 85:6571–6575.

Kaplan, J. H., B. Forbush, and J. F. Hoffman. 1978. Rapid photolytic release of adenosine 5′-triphosphate from a protected analogue: utilization by the Na:K pump of human red blood cell ghosts. *Biochemistry.* 17:1929–1935.

Kratje, R. B., P. J. Garrahan, and A. F. Rega. 1985. Two modes of inhibition of the Ca^{2+} pump in red cells by Ca^{2+}. *Biochim. Biophys. Acta.* 816:365–378.

MacLennan, D. H., C. J. Brandl, B. Korczak, and N. M. Green. 1985. Amino-acid sequence of a Ca^{2+} and Mg^{2+}-dependent ATPase from rabbit muscle sarcoplasmic reticulum, deduced from its complementary DNA sequence. *Nature.* 316:696–700.

MacLennan, D. H., T. Toiyofuku, and J. Lytton. 1992. Structure-function relationships in sarcoplasmic or endoplasmic reticulum type Ca^{2+} pumps. *Ann. NY Acad. Sci.* 671:1–10.

Martell, A. E., and R. M. Smith. 1974. Critical Stability Constants, Vol. 1. Plenum Press, New York.

Maruyama, K., and D. H. MacLennan. 1988. Mutation of aspartic acid-351, lysine-352, and lysine-515 alters the Ca^{2+} transport activity of the Ca^{2+}-ATPase expressed in COS-1 cells. *Proc. Natl. Acad. Sci. USA* 85:3314–3318.

Morgan, K. G. 1993. Ca^{2+}_i versus $[Ca^{2+}]$. *Biophys. J.* 65:561–562.

Pedersen, P. L., and E. Carafoli. 1987a. Ion motive ATPases. *Trends Biochem. Sci.* 12:146–150.

Pedersen, P. L., and E. Carafoli. 1987b. Ion motive ATPases. *Trends Biochem. Sci.* 12:186–189.

Peters, R., J. Peters, K. H. Tews, and W. Bähr. 1974. A microfluorimetric study of translational diffusion in eryhtrocyte membranes. *Biochim. Biophys. Acta.* 367:282–294.

Peters, R., and M. Scholz. 1991. Fluorescence photobleaching techniques. *In* New Techniques of Opitcal Microscopy and Microspectroscopy. R. J. Cherry, editor. MacMillan, New York. 199–228.

Petersen, O. H., C. C. H. Petersen, and H. Kasai. 1994. Calcium and hormone action. *Annu. Rev. Physiol.* 56:297–319.

Press, W. H., S. A. Teukolsky, W. T. Vetterling, and B. P. Flannery. 1992. Numerical Recipes in C. Cambridge University Press, Cambridge.

Scharff, O., and B. Foder. 1978. Reversible shift between two states of Ca^{2+}-ATPase in human erythrocytes mediated by Ca^{2+} and a membrane-bound activator. *Biochim. Biophys. Acta.* 509:67–77.

Schatzmann, H. J. 1966. ATP-dependent Ca^{2+}-extrusion from human red cells. *Experientia.* 22:364–368.

Schwoch, G., and H. Passow. 1973. Preparation and properties of human erythrocyte ghosts. *Mol. Cell. Biochem.* 2:197–218.

Shull, G. E., and J. Greeb. 1988. Molecular cloning of two isoforms of the plasma membrane Ca^{2+} transporting ATPase from rat brain: structural and functional domains exhibit similarity to Na^+, K^+ and other cation transport ATPases. *J. Biol. Chem.* 263:8646–8657.

Strehler, E. E. 1991. Recent advances in the molecular characterization of plasma membrane Ca^{2+} pumps. *J. Membr. Biol.* 120:1–15.

Tsien, R. Y. 1989. Fluorescent indicators of ion concentration. *Methods Cell Biol.* 30:127–156.

Tsien, R. Y., T. Pozzan, and T. J Rink. 1982. Calcium homeostasis in intact lymphocytes: cytoplasmic free calcium monitored with a new, intracellularly trapped fluorescent indicator. *J. Cell Biol.* 94:325.

Verma, A. K., A. Enyedi, A. G. Filoteo, and J. T. Penniston. 1994. Regulatory region of plasma membrane Ca^{2+} pump. *J. Biol. Chem.* 269:1687–1691.

Verma, A. K., A. G. Filoteo, D. R. Stanford, E. D. Wieben, J. T. Penniston, E. E. Strehler, R. Fischer, R. Heim, G. Vogel, S. Mathews, M.-A. Strehler-Page, P. James, T. Vorherr, J. Krebs, and E. Carafoli. 1988. Complete primary structure of a human plasma membrane Ca^{2+} pump. *J. Biol. Chem.* 263:14152–14159.

Zucker, R. S. 1992. Effects of photolabile calcium chelators on fluorescent calcium indicators. *Cell Calcium.* 13:29–40.